CHEMISTRY OF MATERIALS

Communication

pubs.acs.org/cm

Divalent Iron Nitridophosphates: A New Class of Cathode Materials for Li-Ion Batteries

Jue Liu,[†] Xiqian Yu,[‡] Enyuan Hu,[‡] Kyung-Wan Nam,[‡] Xiao-Qing Yang,*[,‡] and Peter G. Khalifah*[,†,‡]

[†]Department of Chemistry, State University of New York at Stony Brook, Stony Brook, New York 11794-3400, United States

[‡]Department of Chemistry, Brookhaven National Laboratory, Uptown, New York 11973, United States

Supporting Information

KEYWORDS: *$Na_2Fe_2P_3O_9N$, $Li_2Fe_2P_3O_9N$, CUBICON, ion-exchange, Li-ion battery, cathode, cyclic voltammetry*

Lithium transition metal phosphates, especially olivine $LiFePO_4$, have been found to be promising rechargeable Li-ion battery cathode materials for many applications since they can safely deliver a good energy density utilizing only earth-abundant materials.[1] However, the olivine materials have limitations which include a poor electrical conductivity[2] and one-dimensional (1D) Li-ion diffusion pathways that can be easily blocked.[3] The search for next-generation phosphate materials has broadened to include transition metal fluorophosphates which incorporate a second anion moiety of F^- and which have good electrochemical performance and favorable intrinsic properties such as 2D ion diffusion channels and small volume changes during ion removal and insertion.[4−6] Here we demonstrate the design of a battery cathode material incorporating N^{3-} anions as a distinct structural building block. While the low mass/charge ratio of N^{3-} is not surpassed by any other anionic group used in battery applications, the voltages previously measured for transition metal nitrides and oxynitrides were low and thus only suitable for anode applications.[7,8] Electrodes with N^{3-} which can deliver suitable voltages for cathode applications have never before been demonstrated. In the present work, it is shown that $A^I_2M^{II}_2P_3O_9N$ compounds with $M^{II} = Fe^{2+}$ and $A^I = Li^+$ can be utilized as cathodes in rechargeable Li-ion batteries. In this structure type, N^{3-} anions are present in the form of nitridophosphate PO_3N tetrahedra that link together MO_6 octahedra.

The compound $Na_2Fe_2P_3O_9N$ (Figure 1) belongs to a class of known compounds with general formula $A^I_2M^{II}_2P_3O_9N$ which are known to exist for A^I = Na and for M^{II} = Mg, Fe, Mn, and Co.[9] Compounds with A^I = Li are clearly of interest for battery applications but have not previously been prepared and could not be directly synthesized under conditions that we have tested due to the preferential formation of olivine $LiFePO_4$, although methods for producing Li-containing nitridophosphate compounds through ion exchange will be demonstrated. Powders of $Na_2Fe_2P_3O_9N$ were synthesized by reacting stoichiometric amounts of $NaPO_3$, Fe_2O_3, and $(NH_4)_2HPO_4$ at 625 °C under flowing NH_3 (50 mL/min) in an open-ended quartz boat for 40 h with one intermediate grinding, similar to prior studies.[9] The full crystal structure of $Na_2Fe_2P_3O_9N$ was determined from the Rietveld refinement of high resolution synchrotron X-ray diffraction data (Figure 2a) and time-of-flight neutron diffraction data (Supporting Information, Figure S1). The expected primitive cubic phase ($P2_13$, No. 198) was observed with a lattice parameter of 9.3459(1) Å, substantially smaller than the 9.40 Å reported originally.[9]

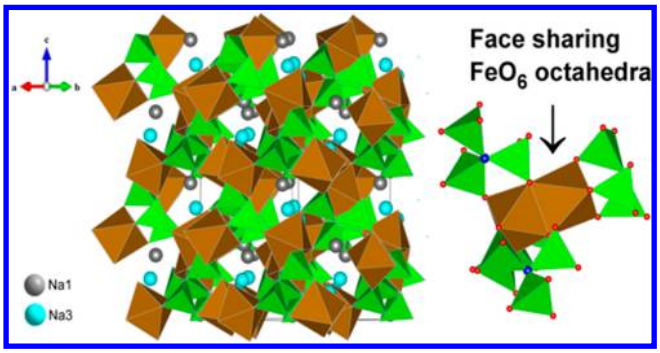

Figure 1. Structure of $Na_2Fe_2P_3O_9N$, with detail showing face-sharing Fe_2O_9 octahedra (brown) and trimeric $P_3O_9N^{6-}$ tetrahedral units (green), with O shown in red and N in dark blue.

The structure of 2:2 $Na_2Fe_2P_3O_9N$ shares the same framework of tetrahedral trimeric $P_3O_9N^{6-}$ anionic blocks as 3:1 $Na_3MP_3O_9N$ analogues (M^{III} = Ti, V, etc.). Although these two structural variants both maintain charge balance for the anionic groups using four cations that are found at the same crystallographic sites, they differ in their ratio of monovalent to multivalent cations (2:2 or 3:1). The additional divalent Fe cation in $Na_2Fe_2P_3O_9N$ occupies an octahedral site that corresponds to the Na2 position in the 3:1 structure type. As a result, the two FeO_6 octahedra in $Na_2Fe_2P_3O_9N$ share a face, as illustrated in Figure 1. This close proximity of the two Fe ions (∼3.0 Å) is expected to strongly influence redox potentials both through electrostatic repulsions and through potentially contradictory bond length preferences for the three shared oxygen ligands that occur when two Fe ions of different valence are found in a single dimer. Full crystallographic parameters (Tables S1−S5) and important bond distances (Table S6) are provided in the Supporting Information.

Received: July 29, 2013
Revised: September 13, 2013
Published: September 18, 2013

 © 2013 American Chemical Society

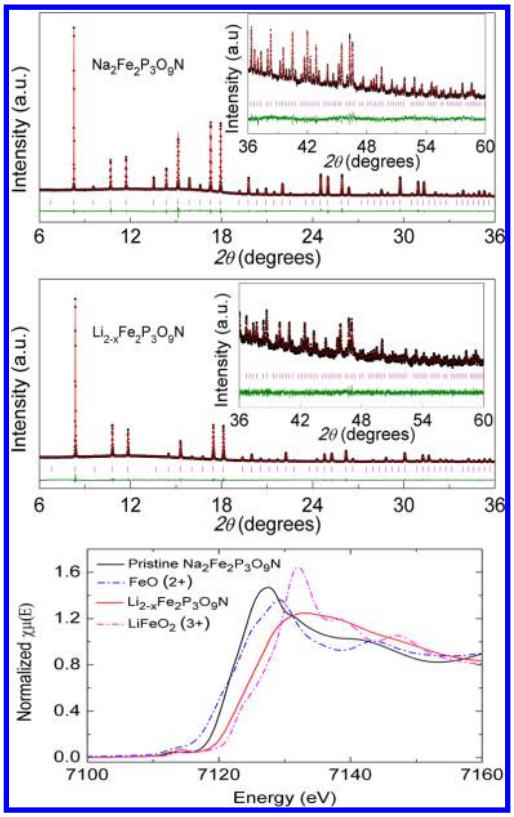

Figure 2. Top: Rietveld refinement of synchrotron diffraction data (λ = 0.7787 Å) of (a) $Na_2Fe_2P_3O_9N$ and (b) the product of its Li-ion exchange, $Li_{2-x}Fe_2P_3O_9N$ with x = 1.7. Bottom: Fe K-edge XANES spectrum of $Na_2Fe_2P_3O_9N$ and $Li_{2-x}Fe_2P_3O_9N$.

The electrochemical performance of $Na_2Fe_2P_3O_9N$ was evaluated in a hybrid-ion configuration (using Li-ion electrolyte and a lithium metal anode) in 2032-type coin cells at room temperature (298 K). To prepare the electrode, $Na_2Fe_2P_3O_9N$ powder was ball milled with carbon black in a 6:3 mass ratio for 30 min prior to coating on an Al current collector with a typical active material loading of 2−3 mg/cm^2. Galvanostatic charge and discharge curves (1.5 V to 4.6 V, C/20) of $Na_2Fe_2P_3O_9N$ indicated that less than one-half of its theoretical capacity of 131 mAh/g could be realized, and that large polarization is present (Supporting Information, Figure S5). These features are both likely the result of low Na^+ mobility within the $Na_2Fe_2P_3O_9N$ lattice. An analysis of bond valence sum difference (ΔV) maps calculated for Na^+ ions within the $Na_2Fe_2P_3O_9N$ lattice (Supporting Information, Figure S7) shows that a very large ΔV threshold of 0.5 valence units must be overcome before a viable Na diffusion pathway is established, suggesting that the removal of Na ions is difficult at room temperature and that low ionic conductivity may be limiting cell performance. This ΔV threshold is much higher than is found[10] for the 3:1 stoichiometry compounds $Na_3VP_3O_9N$ ($\Delta V \sim 0.1$) and $Na_3TiP_3O_9N$ ($\Delta V \sim 0.05$) and likely indicates that Na-ion mobility in this structure family is closely correlated with unit cell dimensions (a = 9.35 Å for M = Fe, 9.45 Å for M = V, and 9.52 Å for M = Ti). In contrast, Li^+ has much smaller ion radii than that of Na^+, suggesting that far better Li-ion kinetics may be observed if all of the Na ions can be chemically removed or replaced by Li^+ prior to electrochemical cell fabrication.

Ion exchange of Li^+ for Na^+ was therefore attempted by heating well ground LiBr and $Na_2Fe_2P_3O_9N$ powders at 280 °C for 20 h under flowing N_2 gas. The resulting mixture was washed with methanol and filtered. This process was repeated (3 times) until the starting phase disappeared (as judged by XRD), giving a final product of a reddish black $Li_{2-x}Fe_2P_3O_9N$ powder. The removal of Na^+ ions was confirmed by a comparison of SEM−EDX spectra before and after ion exchange (Supporting Information, Figure S4), which found that the Na signal was reduced to less than 1% of its original value. Diffraction studies showed that the simple cubic lattice is maintained throughout the exchange process and that the a-lattice parameter shrinks to 9.2565(1) Å. The Rietveld refinement of high resolution synchrotron XRD data confirmed the removal of Na^+ ions from both sites (Na1 and Na3), though only a small amount of Li was inserted into the structure leading to a refined composition of $Li_{0.3}Fe_2P_3O_9N$ and indicating that the final product was oxidized during the ion exchange process. Full crystallographic parameters and relevant bond lengths are provided in the Supporting Information. Electron density corresponding to Li ions was only observed near the Na3 site and not near the Na1 site. The new Li3 site is located close to three oxygen ions with a refined bond distance of 1.89(1) Å, a result which is consistent with the bonding preferences of Li (BVS value of 0.96)[11] and which is in clear contrast to the original Na3−O bond lengths (2.36 Å). Confirmation of this site was obtained through the Rietveld refinement of time-of-flight neutron diffraction data (Supporting Information), though with less precision due to the poorer counting statistics of the experiment. Fe K-edge XANES spectra of $Li_{2-x}Fe_2P_3O_9N$ (Figure 2c) clearly indicates very substantial oxidation during ion exchange, in agreement with the Rietveld results. The sample oxidation during ion exchange is reflected in ∼0.05 Å shorter Fe−O bond lengths at both Fe sites. Curiously, the Fe1 bond lengths are about 0.05 Å shorter than those of Fe2 both before and after oxidation, perhaps reflecting substantial differences in ligand bonding at these two sites.

The calculated bond valence sum difference map for Li-ions suggests the existence of isotropic three-dimensional Li-ion diffusion channels within $Li_{2-x}Fe_2P_3O_9N$ structure which are accessible at a very small observed ΔV threshold of 0.03 vu. On the basis of the BVS analysis, much better battery performance is expected for Na-free compounds $Li_{2-x}Fe_2P_3O_9N$, which were prepared by ion exchange. The voltage charge−discharge profiles of $Li_{2-x}Fe_2P_3O_9N$ cathodes cycled against Li^+/Li at C/10 are shown in Figure 3a and indeed show greatly improved performance relative to $Na_2Fe_2P_3O_9N$ cathodes.

Since $Li_{2-x}Fe_2P_3O_9N$ is mostly oxidized during the ion-exchange process, it was first discharged to intercalate Li^+ into the structure with a measured initial discharge capacity of 100 mAh/g that corresponds to about 1.4 Li^+ inserted into the structure. In subsequent cycles, specific discharge capacities of 125 mAh/g are achieved, corresponding to 85% of the theoretical capacity of 142 mAh/g (1.7 Li^+ per f.u.) of $Li_{0.3}Fe_2P_3O_9N$. A capacity of about 110 mAh/g remains after 20 cycles. In cyclic voltammetry studies (Figure 3b), two separate redox potentials are observed at 3.55 V/3.5 V and 3.1 V/2.95 V. The higher potential occurs at about 3.5 V, indicating that the PO_3N groups in the structure generate a strong inductive effect, which is comparable to that produced by PO_4 groups in $LiFePO_4$. The lower potential of the second couple is attributed to antagonistic effects between the two distinct Fe sites mediated by the three face-shared O anions. The small shifts in

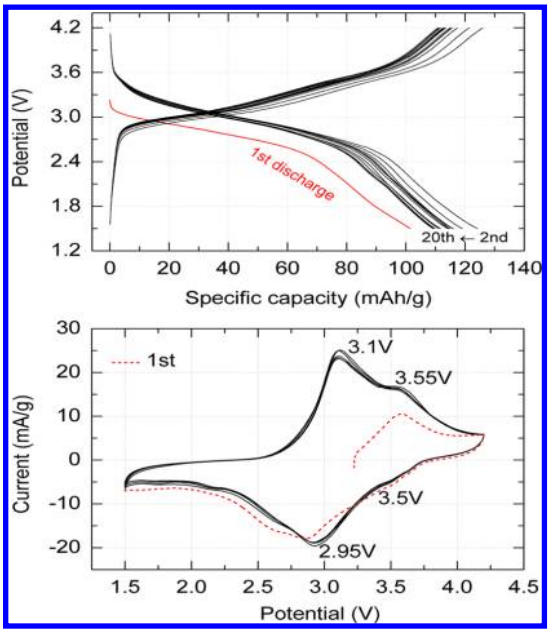

Figure 3. (a) Charge−discharge profiles of $Li_{2-x}Fe_2P_3O_9N$ cycled against a Li anode at a rate of C/10. The theoretical capacity of $Li_2Fe_2P_3O_9N$ is 142 mAh/g. (b) CV curves of $Li_{2-x}Fe_2P_3O_9N$ coin cell (sweep rate: 0.18 V/h).

potential between anodic and cathodic cycles are indicative of reasonable kinetics for these processes, something that can be seen in more explicit rate performance tests (Supporting Information, Figure S6). This performance was achieved with relative large particles (∼1 μm size, Supporting Information, Figure S4), so it is expected that this system has good intrinsic properties and that nanoscale particles will exhibit better rate performance.

In conclusion, we have demonstrated that oxynitrides can be utilized as Li-ion battery cathodes. The transport of Na ions within the cubic $A^{I}{}_2M^{II}{}_2P_3O_9N$ framework is possible but difficult. However, Li^+ transport appears to be facile and nearly the full $Li_2Fe_2P_3O_9N$ theoretical specific capacity of 142 mAh/g (∼140 Wh/L) is accessible after ion exchanging Li^+ for Na^+. One Li^+ site has been located using diffraction data; the position of the second Li^+ site remains to be resolved. The novel nitrophosphate chemistry that we have described therefore represents a promising design strategy for finding new cathode materials for rechargeable Li-ion or Na-ion batteries, as novel compounds with isolated $[PO_3N]^{4-}$ or $P[O_2N_2]^{5-}$ tetrahedral building blocks may have theoretical capacities exceeding 200 mAh/g.

■ ASSOCIATED CONTENT

Ⓢ Supporting Information

Neutron diffraction data, SEM images, EDS spectra, CV and charge−discharge profiles of $Na_2Fe_2P_3O_9N$/Li, C-rate dependence of $Li_xFe_2P_3O_9N$/Li specific capacity, and BVS difference maps. This material is available free of charge via the Internet at http://pubs.acs.org.

■ AUTHOR INFORMATION

Corresponding Authors

*E-mail: xyang@bnl.gov (X.-Q.Y.).
*E-mail: kpete@bnl.gov (P.G.K.).

Notes

The authors declare no competing financial interest.

■ ACKNOWLEDGMENTS

Research was supported as part of the Northeastern Center for Chemical Energy Storage (NECCES), an Energy Frontier Research Center funded by the U.S. Department of Energy, Office of Basic Energy Sciences, under Award DE-SC0001294, including matching support from NYSTAR-NYSDED. This research utilized the facilities at the Center for Functional Nanomaterials and the National Synchrotron Light Source, Brookhaven National Laboratory, which is supported by the U.S. Department of Energy, Office of Basic Energy Sciences, under Contract No. DE-AC02-98CH10886. Research conducted at ORNL's Spallation Neutron Source was sponsored by the Scientific User Facilities Division, Office of Basic Energy Sciences, U.S. Department of Energy. The authors thank Dr. Jianming Bai for beamline X14A assistance, Dr. Yuri Janssen for discussions on and implementation of BVS maps, Dr. Mikhail Feygeson and Dr. Jörg Neuefeind for NOMAD beamline assistance, and Ms. Bingfei Cao for neutron data collection.

■ REFERENCES

(1) Padhi, A. K.; Nanjundaswamy, K. S.; Goodenough, J. B. *J. Electrochem. Soc.* **1997**, *144*, 1188.
(2) Chung, S. Y.; Bloking, J. T.; Chiang, Y. M. *Nat. Mater.* **2002**, *1*, 123.
(3) Li, J.; Yao, W.; Martin, S.; Vaknin, D. *Solid State Ionics* **2008**, *179*, 2016.
(4) Barker, J.; Saidi, M. Y.; Swoyer, J. L. *Electrochem. Solid-State Lett.* **2003**, *6*, A1.
(5) Ellis, B. L.; Makahnouk, W. R. M.; Makimura, Y.; Toghill, K.; Nazar, L. F. *Nat. Mater.* **2007**, *6*, 749.
(6) Barker, J.; Gover, R. K. B.; Burns, P.; Bryan, A. *Electrochem. Solid-State Lett.* **2005**, *8*, A285.
(7) Nishijima, M.; Tadokoro, N.; Takeda, Y.; Imanishi, N.; Yamamoto, O. *J. Electrochem. Soc.* **1994**, *141*, 2966.
(8) Cabana, J.; Rousse, G.; Fuertes, A.; Palacin, M. R. *J. Mater. Chem.* **2003**, *13*, 2402.
(9) Conanec, R.; Feldmann, W.; Marchand, R.; Laurent, Y. *J. Solid State Chem.* **1996**, *121*, 418.
(10) Liu, J.; Chang, D. H.; Janssen, Y.; Yu, X. Q.; Zhou, Y. N.; Bai, J. M.; Ko, J.; Nam, K.-W.; Wu, L. J.; Zhu, Y. M.; Ammatucci, G.; Van de Ven, A.; Yang, X.-Q.; Khalifah, P. G. To be published
(11) Brese, N. E.; Okeeffe, M. *Acta Crystallogr., Sect. B* **1991**, *47*, 192.